Acta Cryst. (1972). A**28**, 560

The Structure of Liquids as Revealed by the Analysis of Their Radial Distribution Functions*†

By S. N. Bagchi

Physics Department, Loyola of Montreal, Montreal, Canada

(*Received* 20 *January* 1972 *and in revised form* 17 *May* 1972)

Published data on radial distribution functions of liquid argon and of many cubic face-centred and body-centred liquid metals at different temperatures (as well as of solid copper at two different temperatures) have been analysed by the method proposed earlier [Bagchi (1970). *Advanc. Phys.* **19**, 119]. Analysis of the results shows that the liquid state consists of clusters of distorted microcrystallites whose linear dimensions vary from 50 to 150 Å. Relative lattice distortion near the melting point is around 10% for f.c.c. structures and 8% for b.c.c. structures. It is shown that from the standpoint of diffraction theory such a structure of the liquid state is equivalent to the two-phase model underlying the significant structure theory of liquids proposed by Eyring and coworkers. Thus the liquid state represents an assembly of small thermodynamic systems. It is suggested that the first order phase transition is caused chiefly by the breakdown of a statistically homogeneous assembly of atoms representing crystals and gases into a statistically inhomogeneous system.

1. Introduction

In practice the radial distribution function (RDF), $g(r)$, is always obtained from the inverse transform of the intensity function (1) derived first by Zernike & Prins (1927)

$$\bar{I}(u)=\bar{N}(V)\times\left[\overline{|f_0|^2}+\overline{|\bar{f}_0|^2|D_0|^2}\,\frac{2}{u}\int_0^\infty rg_0(r)\sin 2\pi ur\,\mathrm{d}r\right]. \quad (1)$$

The function g at different values of r is usually calculated from the relation (2):

$$4\pi r^2g(r)=4\pi r^2\bar{\rho}+8\pi r\int_0^\infty u\,.\,i(u)\sin 2\pi ur\,\mathrm{d}u\,. \quad (2)$$

Here $u=|\mathbf{b}|=2(\sin\theta)/\lambda$ is the magnitude of the reciprocal distance vector $\mathbf{b}$ and r that of the distance vector $\mathbf{x}$ in physical space. $\bar{N}(V)$ is the average number of atoms (or molecules) in the volume V exposed to the primary beam. $\bar{\rho}$ is the average macroscopic density of the liquid. $|f_0|^2$ is the structure factor of the atom (or molecule). $|D_0|^2$ is the Debye–Waller factor due to harmonic thermal vibrations of atoms.

$$i(u)=\frac{\bar{I}(u)-\bar{N}\overline{|f_0|^2}}{\bar{N}\overline{|f_0^2|}}\,, \quad (3)$$

$$g(r)=g_0(r)+\bar{\rho}=\bar{\rho}n_2(r)\,, \quad (4)$$

and $n_2(r)$ = pair distribution function. The symbol ... denotes the value of the function averaged over all directions of space. In order to analyse $g(r)$ properly and to draw reliable conclusions from such analyses, one must first take note of the inherent limitations of (1) and the true physical meaning of $g(r)$ given by (2). In previous publications (see in particular, Hosemann & Bagchi (1962); Bagchi (1970), cited hereafter as I and II respectively) these problems have been discussed in detail from the standpoint of the Unified Kinematic Theory of Diffraction by Matter of Any Kind. Since in this paper we shall be using this theory to analyse $g(r)$ obtained from (2) and to draw many new conclusions, it is desirable that we look at this unified theory and its relations to the conventional theories – [namely, (i) Laue–Bragg–Debye–Waller theory of diffraction by crystals, (ii) the theory of scattering by 'primitive' liquids as formulated by Zernike & Prins and Debye & Menke and (iii) the theory of scattering by ideal gases or amorphous matter developed by Debye, Guinier and others, which for variety of reasons are almost always used for practical evaluation of the results of diffraction experiments] – from the standpoint of distribution function theory.

The intensity function $I(\mathbf{b})$ coherently scattered in the Fraunhofer region by any system whatsoever, (homogeneous or inhomogeneous), is given, apart from proportionality factors which depend on the experimental set up but not on the density distribution encountered in the system, by

$$I(\mathbf{b})=\sum_{m=1}^{N}\sum_{n=1}^{N}f_mf_n^*\exp\{-2\pi i[\mathbf{b}\,.\,(\mathbf{x}_m-\mathbf{x}_n)]\}\,, \quad (5)$$

where $f_m(\mathbf{b})$ is the scattered amplitude for the electron density distribution of the mth atom when its centroid lies at the origin, $f_n^*(\mathbf{b})$ is the complex conjugate of the scattered amplitude for the nth atom and $\mathbf{x}_m-\mathbf{x}_n$ is the distance of separation of these two atoms, $\mathbf{b}$ is the reciprocal vector defined by $\mathbf{b}=\boldsymbol{\sigma}-\boldsymbol{\sigma}_0/\lambda$; $|\mathbf{b}|=2\sin\theta/\lambda$,

---

* Part of the lecture delivered at The Second International Conference on Small Angle Scattering held at Graz (Austria) in August, 1970.

† This work was supported by The National Research Council of Canada.

σ, σ_0 are unit vectors in the directions of scattered and incident beams respectively; λ is the wavelength of the incident beam, 2θ is the scattering angle and N is the number of atoms present in the substance.

The expression (5), though exact, is for all practical purposes useless. In order to get a useful expression out of this one always uses the probability of occurrence of the mth atom with respect to the reference atom and sums over all the atoms m and n. It must be noted that this probability and summation refer to the atoms in the physical space and consequently, should be introduced in the appropriate expression for the density distribution and not in equation (5). If one intends to introduce the averaging over all positions of atoms in equation (5), one has to incorporate the 'pair distribution function' and not the density distribution of centroids of atoms. This pair distribution function is proportional to the convolution square of the density function. Consequently, neither from intensity data nor from its inverse transform do we get this probability function *directly*. Conventional theories mentioned above are obtained by assuming different probability distribution functions for the occurrence of the atoms. In all such theories one is forced to introduce the concept of distribution function for the occurrence of atoms relative to any origin in order to get any useful information out of the generally valid expression (5). This means that all conventional theories are applicable to systems which are statistically homogeneous. Obviously none of these theories can offer us dependable results if the system is statistically inhomogeneous. It is therefore obvious that in order to get a generally valid expression for the intensity function which would yield the well known expressions of the conventional theories, one must restrict oneself to substances which are statistically homogeneous. From the detailed considerations of the intensity function of any arbitrary structure it was proved before (*cf.* references I and II) that for this it is necessary to introduce the concept of a *generalized* lattice. A generalized lattice need not be a perfectly periodic pattern but has to prescribe the reference points of the lattice with given *a priori* statistics. For this it is necessary and sufficient that we define the generalized lattice as a statistically homogeneous system in which the volumes of the lattice cells are distributed randomly for *any* volume under consideration. Consequently, not only volumes of lattice cells in a generalized lattice vary independently both in their shapes and sizes, but the reference points of lattice cells are also distributed randomly throughout the space. The statistics of neighbouring lattice points inform us about the degree of distortion of the

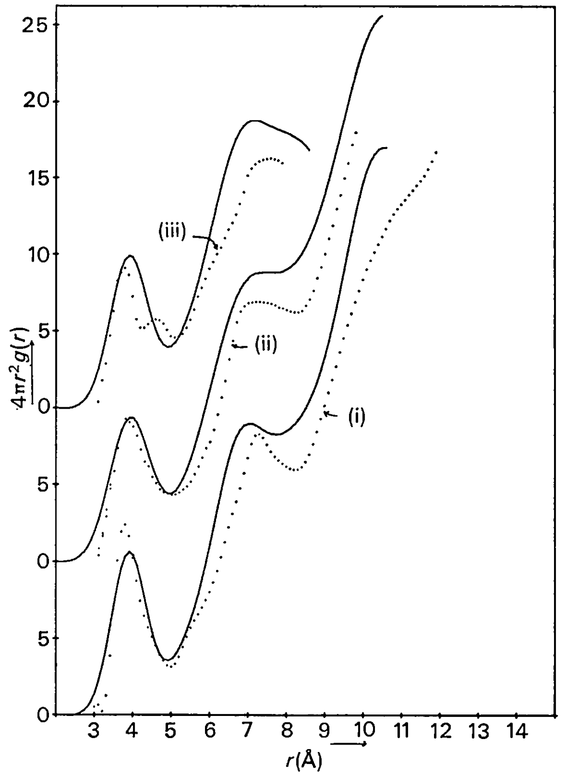

Fig. 1. Liquid argon. (i) Ar–1 at 84·25°K (Gingrich & Thompson, 1962), (ii) Ar–H at 84°K (Henshaw, 1957), (iii) Ar–2 at 91·8°K (Eisenstein & Gingrich, 1942). (Vertical scales are successively shifted by 10 units). Experimental (. . .) and calculated (—) RDF by varying α only.

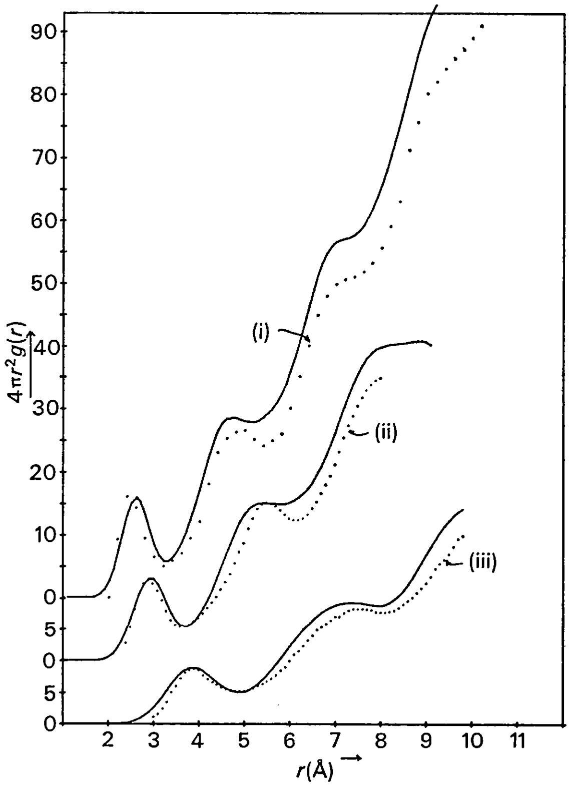

Fig. 2. (i) Liquid copper at 1313°K (Ruppersberg, 1964), (ii) Liquid gold at 1373°K (Hendus, 1947), (iii) Liquid sodium at 373°K (Gingrich & Heaton, 1961). (Vertical scales are successively shifted by 10 units). Experimental (. . .) and calculated (—) RDF by varying α only.

ideal lattice and the generalized lattice depending on this degree of distortion could represent the structures not only of crystals, liquids and gases but also of any (statistically) homogeneous substance provided we distribute the atoms around these reference points.* The Fourier transform of the distance statistics of these reference points, the so-called lattice statistics z (**x**), then describes the characteristic features of diffraction patterns not only for ideal crystals, primitive liquids and ideal gases, but also for any substance in any state of aggregation provided it is statistically homogeneous.

The intensity function $I(\mathbf{b})$ and its inverse transform $Q(\mathbf{x})$ for any statistically homogeneous substance can be expressed as (see II, equations 48–50):

$$\bar{I}(\mathbf{b}) = \bar{N}(V)\,[\overline{|f_0|^2} - |D_0|^2|\bar{f_0}|^2] + \frac{1}{\bar{v}}\,|D_0|^2|\bar{f_0}|^2\{Z * |S|^2\}\,, \quad (6)$$

$$\bar{Q}(\mathbf{x}) = \bar{N}(V)\left[\overline{\overset{2}{\tilde{\rho}}}_0 - \overset{2}{\tilde{A}}_0 * \overset{2}{\tilde{\bar{\rho}}}_0\right] + \frac{1}{\bar{v}}\,\overset{2}{\tilde{A}}_0 * \overset{2}{\tilde{\bar{\rho}}}_0 * \left[z\overset{2}{\tilde{s}}\right] \quad (7)$$

where $\bar{v}$ = the mean volume of the primitive lattice cell or, the mean volume occupied by a 'particle', $\rho_0(\mathbf{x})$ = cell element *i.e.* density distribution function within the elementary cell with its centroid at the origin, $s(\mathbf{x})$ is Ewald's shape function and $S(\mathbf{b})$ its Fourier transform, $f_0(\mathbf{b}) = \mathscr{F}\rho_0(\mathbf{x})$ and

$$z(\mathbf{x}) = \lim_{N\to\infty} \frac{1}{N} \sum_{n,} \sum_{m=1}^{N} \delta(\mathbf{x} - \mathbf{x}_m + \mathbf{x}_n) \quad (8)$$

is the lattice statistics, *i.e.* distance statistics function within a single infinitely extended lattice.

Also $Z(\mathbf{b})$ = lattice statistics factor $= \mathscr{F}z(\mathbf{x})$; $\mathscr{F}$, $\mathscr{F}^{-1}$ are the symbols of Fourier integrals; dv_x, dv_y are elements of volume in the physical space; dv_b is the volume element of the reciprocal space, $*$ is the symbol for convolution product and $\tilde{2}$ that for convolution square, *i.e.* convolution product of a function $g(\mathbf{x})$ and its inverse symmetric function $g(-\mathbf{x})$.

$A_0(\mathbf{x}) = \overline{A_p(\mathbf{x})} = \overline{\delta(\mathbf{x} - \Delta x_p)}$; $D_0(\mathbf{b}) = \mathscr{F}A_0(\mathbf{x})$. $A_0(\mathbf{x})$ represents the distribution of the centroid of the cell element $\rho_{0p}(\mathbf{x})$ lying at the pth cell around its mean value $\mathbf{x}_p$. Let us note here that the distribution function $A_0(\mathbf{x})$ which represents the deviation of the centroid of the atoms from their most probable values really splits up the statistical distribution of atoms due to anharmonic vibrations into the distribution of most probable positions of the atoms and the distribution of the centroids of the atoms around these positions, analogous to the so-called quasi-harmonic approximation of crystal lattice vibrations. Only in this case most probable positions, *i. e.* the reference points of the generalized lattice, are distributed in a characteristic way depending on the structure instead of in an ideal lattice. It includes the distortion of the first kind as defined before (see I and II) as a special case. In the more general case it is merely a convenient way of describing the statistical distribution of the centroids of atoms within the system. Consequently, as will be seen later, in analysing RDF of liquids it is enough to determine the degree of lattice distortion, *i.e.* the distribution of the most probable positions of the lattice cells as well as their dispersions around these values. The effect of thermal vibration is completely included in this expression and our experience shows that it would give wrong results if in analysing RDF we try to separate them arbitrarily into first kind, due to thermal vibrations alone and the second kind due to lattice positions. The correct procedure for getting the information about these two kinds of distortions is described with reference to equations (16) to (19).

It is to be noted that contrary to the expression of the intensity function of an arbitrary structure, the expression (6), whose characteristic features depend chiefly on $Z(\mathbf{b})$, can be analysed quantitatively with the help of a few coordination statistics. For 'primitive' liquids only one spherically-symmetric-nearest-neighbour statistics is sufficient to characterise $Z(\mathbf{b})$, (for the proof see reference II, section 9).

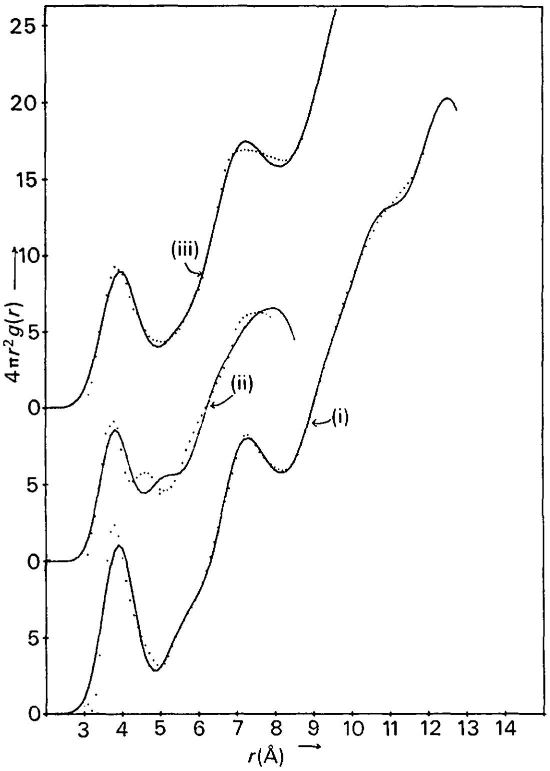

Fig. 3. (i) Ar–1, (ii) Ar–2, (iii) Ar–H. (Vertical scales are successively shifted by 10 units). Experimental (. . .) and calculated (—) RDF by varying all parameters *simultaneously*.

---

* For theoretical treatment we can always consider a primitive lattice; the density distribution within an atom would then constitute the cell element ϱ_0 (**x**) of the lattice.

Further, as has been proved before, equation (6) not only degenerates to the well known expressions of the conventional theories, but also predicts something more. It defines the conditions which would produce reflexions characteristic of each of these types and the limits of the validities of each of them. For example, if

$$\Delta Z(\mathbf{b}-\mathbf{b}_h)>>>\Delta|S(\mathbf{b}-\mathbf{b}_h)|^2,\dagger \tag{9}$$

equation (6) reduces to the expression (10)

$$\bar{I}(\mathbf{b})=\bar{N}(V)\,[\overline{|f_0|^2}+|\bar{f}_0|^2|D_0|^2(Z-1)]\,, \tag{10}$$

which shows 'diffuse' reflexions having all the characteristic properties of the intensity distribution scattered by a liquid.

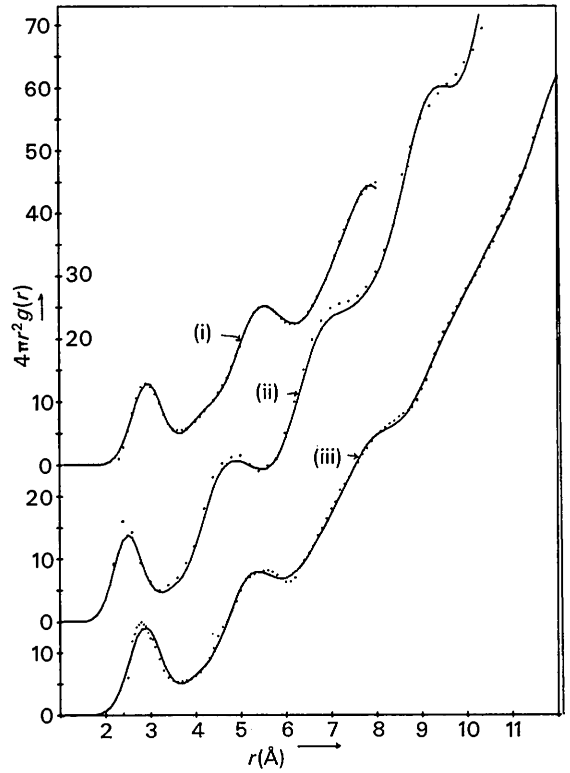

Fig. 4. (i) Liquid gold, (ii) Liquid copper (Vertical scale shifted by 25 units). (iii) Liquid aluminum at 943 °K (Ruppersberg, 1965). (Vertical scale shifted by a further 15 units). Experimental (. . .) and calculated (—) RDF by varying all parameters *simultaneously*.

Moreover, if the distance statistics $z(\mathbf{x})$ is spherically symmetric, its Fourier transform would also be spherically symmetric and equation (10) in this case reduces to the well-known expression (1). The function $g(r)$ is related to $z(\mathbf{x})$ by (11):

$$g(r)=g_0(r)+\frac{1}{\bar{v}}=z(\mathbf{x})-\delta(\mathbf{x}-0)=\bar{p}n_2(r);\ \left(\bar{p}=\frac{1}{\bar{v}}\right). \tag{11}$$

It is important to note that since $Z(\mathbf{b})$ contains a delta function of weight $1/\bar{v}$ at $\mathbf{b}=0$, $Z(\mathbf{b})$ always behaves like a delta function compared to $|S|^2$ as $\mathbf{b}\rightarrow 0$. Consequently, equation (10) and, therefore, equation (1) are not applicable in the neighbourhood of $\mathbf{b}=0$. That means, as is well known, the central reflexion *i.e.* 000-reflexion, is *always crystalline* no matter what is the degree of lattice distortion and it is not contained in the expressions (10) and (1).

2. Distance statistics function $z(\mathbf{x})$ and correlation length

The distance statistics function $z(\mathbf{x})$ is defined by the expression (8). It shows that the function $z(\mathbf{x})$ gives the

---

† Δ represents the widths of the humps of the functions. Symbol > > > indicates greater in all three directions.

Table 1. *Significant structural parameters, e.g. lattice distortion, correlation lengths for simple liquid systems as well as for solid copper at two different temperatures having f.c.c. crystalline structures obtained from the analysis of their radial distribution functions*

For the exact meaning of the symbols and their derivation, see text (§ 3).

	Ar–H	Ar–1	Ar–2	Al	Au	Pb		Cu		
T(°K)	84	84·4 (0·8 atm)	91·8 (1·8 atm)	943	1373	623	823	1313	1293	973
Θ(°K)	80	80	80	396	186	86	86	313	313	313
α	0·6678	0·5965	0·5381	0·4979	0·4785	0·5904	0·6054	0·4378	0·2802	0·2210
r_1	3·861	3·861	3·746	2·813	2·891	3·388	3·390	2·462	2·563	2·527
Δ^2r	0·2230	0·1779	0·1448	0·1240	0·1146	0·1743	0·1833	0·0958	0·0393	0·0244
$\Delta r/r_1$ (%)	12·23	10·92	10·16	12·51	11·70	12·32	12·63	12·57	7·73	6·18
$\lvert p_c\rvert$ (n.d.)	17	21	24	16	18	17	16	16	42	65
L_c (Å)	16·39	18·21	19·10	11·60	12·60	13·97	13·56	10·15	17·57	21·44
Δ^2s	0·0487	0·0487	0·0487	0·0323	0·0291	0·0619	0·0798	0·0305	0·0300	0·0227
Δ^2a	0·1743	0·1292	0·0961	0·0917	0·0855	0·1124*	0·1035*	0·0653	0·0093	0·0017
$\Delta a/r_1$ (%)	10·85	9·31	8·28	10·76	10·11	9·896*	9·490*	10·38	3·76	1·63
$\lvert p_l\rvert$ (n.d.)	86	115	146	86	98	103*	112*	93	706	3765
L (Å)	75·7	89·4	95·4	55·1	67·4	68·76	71·75	50	≈143	≈325

* The slight differences in the numerical values should not be considered as significant. The reversed order for higher temperatures is more likely due to the inaccuracy in the values of Δ^2s calculated from Debye's theory for harmonic vibrations and uncertainties involved in the values for Θ.

average distances of the centroids of different neighbours of an identical structure but extended indefinitely. It must be noted that this averaging is obtained conceptually by measuring the distances of each neighbour with respect to a fixed centre and then taking each centre as the reference point and finally averaging over all centres. This is easily seen if we note that the expression

$$z_n(\mathbf{x}) = \sum_{m=1}^{N} \delta(\mathbf{x} - \mathbf{x}_m + \mathbf{x}_n)$$

gives the distances of all the particles m from the fixed nth atom. Further, since $\delta(\mathbf{x}-\mathbf{x}_m+\mathbf{x}_n)=\delta(\mathbf{x}-\mathbf{x}_m) * \delta(\mathbf{x}-\mathbf{x}_n)$, the distance statistics function (8) really is the convolution product of the density distribution and does not directly give the density distribution. Even for a substance containing 'point-like' atoms (*i.e.* atoms whose density distribution is given by delta functions) the inverse transform of the intensity function does not give the distances between the atoms directly, though in such simple cases the Q function is directly proportional to $z(\mathbf{x})$:

$$\mathscr{F}^{-1} I(\mathbf{b}) \equiv Q(\mathbf{x}) = 1/\bar{v} \,.\, z(\mathbf{x}) \,.\, \overset{2}{\tilde{s}}(\mathbf{x}). \qquad (12)$$

The function $z(\mathbf{x})$ contains a delta function of weight unity at $\mathbf{x}=0$ and vanishes (for rigid atoms) within a distance of twice the radius of the atom. At larger distances it shows maxima and minima characteristic of the distribution and finally at a sufficiently large distance, again characteristic of the distribution function, it attains a constant value equal to the average density. The interaction zone of the distribution therefore extends to the region v_l where the function $z(\mathbf{x})$ has not yet reached its final constant value $1/\bar{v}$ and it is usually designated as the 'correlation length' of the distribution. From physical considerations it is evident that the correlation length must always be finite if the distances of neighbours show the slightest fluctuation. Once we have the coordination statistics we can estimate the radius of the interaction zone, *i.e.* the correlation length of the lattice as well as that of the pair distribution function. The number of nearest neighbours in a particular direction $\mathbf{k}$ corresponding to these two correlation lengths are obtained respectively from the formulae

$$|p_l| = |\bar{\mathbf{a}}_\mathbf{k}|/(\Delta_k^2 x)_{\text{lattice}}\,, \qquad (13)$$

$$|p_c| = \varepsilon^2 \,.\, |\bar{\mathbf{a}}_\mathbf{k}|^2/(\Delta_k^2 x)_{\text{total}}\,, \qquad (14)$$

where $(\Delta_k^2 x)_{\text{lattice}}$ and $(\Delta_k^2 x)_{\text{total}}$ denote respectively the mean square fluctuation in the positions of atoms due to lattice distortion alone and to the joint effect of the lattice distortion and thermal vibrations. For details see § 3. ε is a parameter which determines the zone in Fourier space, the so-called limiting ellipsoid of reflexion, outside which no distinct reflexion hump can be observed. The value of ε depends on the coordination statistics, (for proof see reference II, § 11).

3. Analysis of $g(r)$ of simple liquids

The function $g(r)$ is calculated from the expression (2) and is based on the intensity function (1) of the Zernike–Prins theory. Consequently, as noted before, neither equation (10) nor equation (1) is generally valid in the domain of small-angle scattering. If the small-angle scattering does not extend to the region of interest and if the observed intensity function is corrected for other relevant factors, *e.g.* incoherent scattering, absorption factor, termination effect, *etc.*, then, equations (10) and (1) are correct for 'primitive' liquids, *i.e.* liquids which can be looked upon as a single statistically homogeneous lattice. From equation (2) we shall therefore get the correct $g(r)$ provided the structure factor $|f_0|^2$ is known. The ratio $|D_0|^2 \,.\, |\bar{f}_0|^2/\overline{|f_0|^2}$ is absorbed in $i(u)$, [*cf.* equation (10)], so that $g(r)$ includes also the smearing effect of the random thermal vibrations of the atoms. It means that $g(r)$ contains effects of distortion of the lattice and of (random) thermal vibrations. Both these effects simultaneously determine the correlation length of the pair distribution function. Since even in crystals distances of nth and $(n+1)$th neighbours $(n \gg 1)$ lie very close to one another, due to thermal vibrations, $g(r)$ functions would attain their final

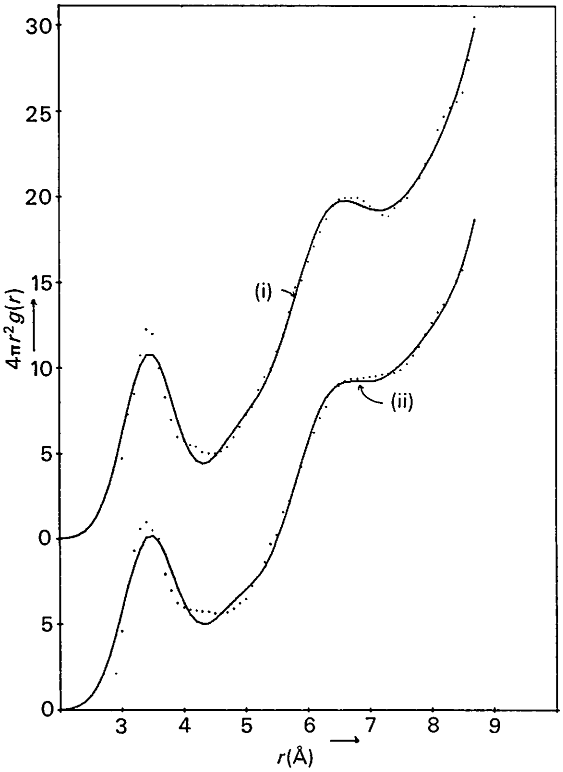

Fig. 5. Liquid lead (Sharrah & Smith, 1953). (i) at 623°K, (ii) at 823°K. (Vertical scale shifted by 10 units). Experimental (...) and calculated (—) RDF by varying all parameters *simultaneously*.

constant value after a relatively short distance. This means, that the 'correlation length' $|p_c|$ of $n_2(r)$, even for crystals, would be (relatively) quite short, (see the values for Cu at 973 and 1293 °K in Table 1). But one must be cautious in applying equation (2) for the case of crystals since equations (10) and (1) and consequently equation (2) are valid *only* if the humps of the shape factor behave as delta functions compared to those of the $Z(\mathbf{b})$ functions. For 'crystals' these equations would be applicable if the linear dimension of the crystallites is greater than the interaction zone of the lattice. That is, if

$$|p_{lk}| > \frac{|\bar{\mathbf{a}}_{\mathbf{k}}|^2}{\Delta_k^2 a}, \quad [cf. \text{ equation } (13)].$$

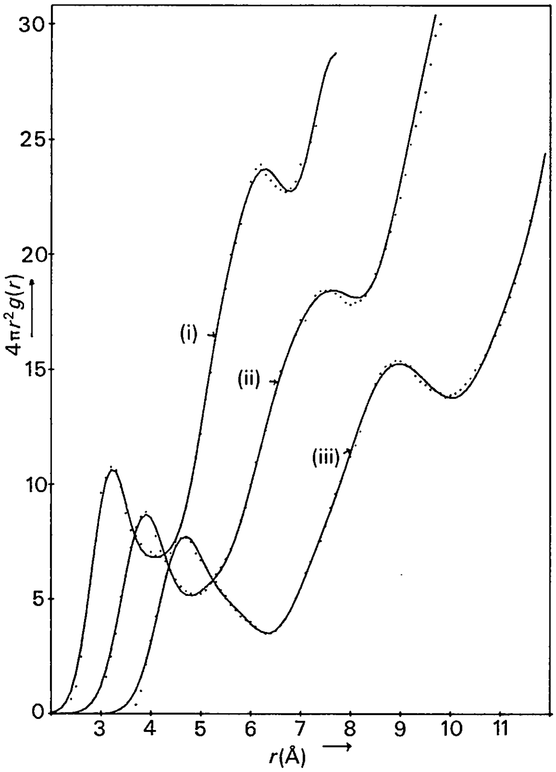

Fig. 6. (i) Liquid lithium at 453 °K, (ii) Liquid sodium at 373 °K, (iii) Liquid potassium at 338 °K. Experimental values (. . .) (Gingrich & Heaton, 1961) and calculated (—) RDF by varying all parameters *simultaneously*.

It is obvious that for 'perfect' crystals equation (2) would not be valid. Of course, for any structure whatsoever, the inverse transform of the intensity function (over the *entire* Fourier space) always gives $z(\mathbf{x})$, but in general it involves the shape factor in a complicated way, [see equation (12)]. Nevertheless, for real crystals at higher temperatures where the lattice distortion becomes considerable (see the data for copper in Table 1) it may be that the relation $\Delta Z(\mathbf{b}) >>> \Delta |S|^2$ is satisfied so that we can apply equation (2). Since we intend to analyse the data already available in this domain, let us assume the validity of equation (2) for crystalline powders at temperatures near their melting points. Kaplow, Averbach & Strong (1964) and Kaplow, Strong & Averbach (1965) had determined $g(r)$ of Pb at 325 and 329 °C, but the data supplied by these authors from a conventional analysis of RDF cannot be relied upon for the following reasons: (i) the $g(r)$ function is not identical with the density function and cannot be analysed by putting Gaussian functions at the observed maxima. (ii) Mean-square displacements are much too large compared to that obtained from Debye's theory. If their values were correct we could get completely wrong results for the specific heats. On the other hand, Debye's method of determining amplitudes of thermal 'harmonic' vibration, though suffering from several limitations, still gives very accurate values of specific heats. (iii) One cannot make inferences about coupled thermal vibration from the results obtained from expressions (1) and (2) which were derived under the fundamental assumption of random thermal vibrations. It is known that coupled vibrations affect only the diffuse background scattering, (though under specific conditions they may lead to

Table 2. *Significant structural parameters for liquid alkali metals (b.c.c. structure) at various temperatures*

For the exact meaning of the symbols and their derivative, see text (§ 3).

	Li	Na	K	Rb				Cs		
T (°K)	453	373	338	313	433	513	633	303	573	848
Θ (°K)	430	160	99	65	65	65	65	39·5	39·5	39·5
α	0·5099	0·6188	0·6355	0·7368	0·9858	0·9902	1·03	0·7693	0·8713	1·011
r_1	3·117	3·789	4·518	4·925	4·741	4·763	4·77	5·284	5·251	5·251
$\Delta^2 r$	0·13	0·1915	0·2019	0·2715	0·4859	0·4902	0·530	0·296	0·3795	0·5105
$\Delta r/r_1$ (%)	11·57	11·54	9·95	10·58	14·70	14·70	15·27	10·3	11·73	13·61
$\|p_c\|$ (n.d.)	19	19	25	22	12	12	11	24	18	14
L_c (Å)	12·98	15·77	22·14	22·75	16·19	16·28	15·58	25·16	21·65	19·18
$\Delta^2 s$	0·0524	0·0919	0·1277	0·1254	0·1735	0·2055	0·2536	0·2113	0·3994	0·591
$\Delta^2 a$	0·0776	0·0996	0·0742	0·1461	0·3124	0·2847	0·2764	0·0847	?*	?*
$\Delta a/r_1$ (%)	8·94	8·33	6·03	7·76	11·79	11·20	11·03	5·5		
$\|p_l\|$ (n.d.)	125	144	275	166	72	80	82	330		
L (Å)	68·7	90·4	≈148	126	79·54	84·32	85·84	≃190		

* The anomalies are more likely due to the errors in the values of $\Delta^2 s$ calculated from Debye's theory for *harmonic* vibrations and the uncertainties in the correct value for Θ rather than to the presence of clusters.

extra Laue spots), and consequently a much more detailed analysis of background scattering is needed to conclude anything about the nature of coupled vibrations. Further, equations (1) and (2) are not generally valid for cases where coupled vibrations play significant roles. Nevertheless, their published curves show convincingly that lattice distortion is present in solid lead as well but is smaller than in the case of liquids. These errors are also involved in the data presented by Ruppersberg (1964, 1965, 1966) in his analysis of aluminum and copper RDF. Our analysis of RDF of copper by Ruppersberg shows definitely that even just below the melting point the lattice distortion is significant but smaller than that in the liquid state. It also decreases markedly with decreasing temperature, (see Table 1). We can therefore conclude that lattice distortion exists at ordinary temperatures and increases appreciably as the temperature approaches the melting point. Nevertheless, at the melting point there is a significant jump in the lattice distortion. We can therefore safely conclude that liquids are nothing but more distorted crystallites of smaller sizes.

We shall now proceed to analyse the available $g(r)$ functions of various simple liquids by the method proposed earlier (reference II). We shall assume that equations (1) and (2) are valid and examine in detail the consequences of this assumption. Since $g(r)$ represents the convolution square of the density function, we have to 'deconvolute' $g(r)$ to get the density distribution. We shall not use the analytic solution but fit the given $g(r)$ curve by choosing properly, by trial and error, the probability distribution of the first neighbour $H_1(r)$. The probability distribution of the nth neighbour is given by

$$H_n(r) = \sum_p H_p(r)\,,$$

$$H_p(r) = \frac{1}{4\pi^{3/2}m^{1/2}\alpha r_p}\;\frac{1}{r}\left\{\exp\left[-\frac{(r-r_p)^2}{m\alpha^2}\right] - \exp\left[-\frac{(r+r_p)^2}{m\alpha^2}\right]\right\}. \quad (15)$$

The summation is to be taken over all the atoms belonging to the given nth neighbour. It is determined by the coordination number C_p. r_p denotes the location of the centroid of the pth atom; $\alpha^2/2 = \Delta^2 r$ denotes the mean-square fluctuation in any direction of the nearest-neighbour distance vector (n.d.) from r_1, its most probable value.* m denotes the number of convolutions by which the pth atom is reached from the origin with the help of uncorrelated fundamental vectors of the nearest neighbours. All values are referred to the corresponding crystal structure at 0°K. Evidently, this corresponds to the case of harmonic displacements of the atoms around their *ideal* lattice positions. Consequently, we should not expect any close agreement with the experimental results by varying α only. Nevertheless, as Figs. 1, 2, 9 (ii) and 9 (iv), show the results are strikingly similar.† Since in general, owing to anharmonic vibrations, r_p's would also vary around their most probable positions and C_p's would also change from their crystalline values due to fissures, holes and clusters present in the liquid state, we did not try to achieve a closer agreement by varying α only. Instead, by varying successively (α, r_p, C_p) we tried to obtain the best possible fit with the curve obtained from experimental results. We have not shown these curves here, but generally the agreement is better when one varies α and r_p simultaneously, keeping C_p constant. This shows that variation of equilibrium positions plays a relatively more important role in determining the $g(r)$ curve. Of course, the best fit is obtained when one varies α, r_p and C_p simultaneously. Figs. 3–8 speak for themselves and completely support our claim that liquids are nothing but distorted crystallites. It might be argued that since we have so many parameters to vary, it is not surprising that the agreement is good. But we have to remember that we are varying the parameters of the underlying crystalline structure. Consequently, there is not much freedom in the choice of parameters. A little trial would show that by arbitrarily varying any parameter, the agreement is largely destroyed.‡

Tables 1 and 2 summarize the results of analysis of RDF by giving the significant structural parameters of the liquid state, namely, α, $\Delta^2 r$, $\Delta^2 a$, $|p_c|$, L_c, $|p_l|$, L.

Table 3. *Most probable positions of various neighbours and their coordination numbers as calculated from the analysis of* RDF *for liquid argon*

For the exact meaning of the symbols and their derivation see text (§ 3).

	Ar–H	Ar–1	Ar–2
r_1; C_1	3·861; 10·245	3·861; 11·605	3·746; 7·87
r_2; C_2	5·38; 6·95	5·665; 8·49	4·98; 6·81
r_3; C_3	6·90; 23·62	7·03; 22·05	6·33; 11·77
r_4; C_4	7·96; 12·53	7·996; 12·00	7·25; 12·84
r_5; C_5	9·27; 23·99	9·25; 25·00	8·28; 23·46
r_6; C_6	9·27; 7·98	9·34; 8·10	
r_7; C_7	10·64; 47·66	10·65; 45·05	
r_8; C_8	10·54; 5·90	12·04; 7·55	
r_9; C_9		12·01; 13·09	
r^1_9; C^1_9		12·23; 24·28	
r_{10}; C_{10}		12·64; 24·43	
r_{11}; C_{11}		13·43; 23·73	
r_{12}; C_{12}		13·78; 13·96	
$\sum^2$	8·10	38·18	21·12

---

* For a normalized spherically symmetric function $f(r-r_p)$,

$$\Delta^2 r = \int_0^\infty (r-r_p)^2 f(r-r_p)\,.\,4\pi r^2 \mathrm{d}r.$$

† They illustrate the differences between $g(r)$ functions due to atomic distributions represented by (crystalline) harmonic vibrations and the observed $g(r)$ functions, satisfactorily reproduced in densely packed systems by harmonic dispersions of atoms around the generalized lattice, (*cf.* Figs. 3–9).

‡ It should be emphasized that one must aim at curve fitting throughout the region and not merely in the neighbourhood of the first peak. The departure at the tail end of the calculated curves is due to the fact that only a finite number of neighbours (usually 8–12) was considered.

Table 4. *Data as for Table* 3 *but for simple liquid f.c.c. metals as well as solid copper at two temperatures*

For the exact meaning of the symbols and their derivation, see text (§ 3).

	Al	Au	Pb		Cu		
			623 °K	823 °K	1313 °K	1293 °K	973 °K
r_1; C_1	2·813; 12·09	2·891; 10·68	3·388; 11·04	3·39; 10·47	2·462; 10·31	2·563; 12·59	2·527; 10·60
r_2; C_2	3·99; 6·36	4·16; 8·72	4·87; 8·36	4·777; 8·35	3·41; 4·46	3·64; 6·08	3·65; 8·03
r_3; C_3	5·09; 23·26	5·24; 22·41	6·176; 22·25	6·198; 22·25	4·43; 18·51	4·52; 26·62	4·41; 26·10
r_4; C_4	5·90; 11·90	5·89; 12·30	7·073; 12·38	7·16; 12·95	5·05; 13·73	5·17; 8·73	5·07; 13·14
r_5; C_5	6·76; 24·47	6·84; 28·02	8·05; 24·03	8·165; 23·64	5·73; 17·35		
r_6; C_6	6·88; 8·01	8·27; 12·83	8·40; 7·89	8·17; 7·99	6·15; 5·92		
r_7; C_7	7·85; 47·5	7·92; 45·6	9·51; 47·8	9·77; 46·6	6·72; 40·7		
r_8; C_8	10·18; 5·9	7·28; 5·70	9·91; 6·0	9·77; 10·6	7·39; 6·7		
r_9; C_9	8·87; 12·0		10·58; 12	10·21; 12	7·63; 10·5		
$r_{9'}$; $C_{9'}$	8·93; 24·0		10·46; 22·0	10·21; 24·2	7·62; 23·0		
r_{10}; C_{10}	9·29; 24·1		10·46; 23·2	10·292; 24·6	8·00; 14·3		
Σ^2	63·02	6·91	16·79	17·57	175·15	67·64	440·27

Tables 3 to 5 give the pertinent values of r_ps and C_ps. $\sum^2$ represents the sum of least squares for about 50–75 equidistant points. We did not consider it worthwhile consuming more computer time to obtain better agreement.

From the curves near the melting points it can be seen that extremely good agreement has been obtained by varying *only the distribution of the centroids of atoms around their most probable positions.* In fact, as pointed out earlier, in the $g(r)$ function only the positions of the atoms, due to the combined effect of lattice distortion and harmonic vibrations around each of the lattice points, constitute the determining factor. These factors jointly determine the correlation length of the $g(r)$ function, *i.e.* of the pair distribution function $n_2(r)$. Further, Figs. 6 to 8 show convincingly that curves for liquid alkali metals near their melting points can be fitted well to distorted body-centred-cubic structures.

In order to find the correlation length L_c of the pair distribution function we determine first the number of neighbours corresponding to it from the formula (14)

$$|p_c| \simeq \varepsilon^2 \, . \, (r_1/\Delta r)^2. \tag{14a}$$

It must be noted that the nth neighbour distance (n.d.) $d_n \neq n \, . \, r_1$, (r_1 = nearest n.d.) but depends on the structure. The mean value $\bar{r}_1 = r_1 + \alpha^2/2r_1$ differs only slightly from the most probable value and we have not tried to distinguish between them. All the relevant values quoted in the Tables 1–5 were calculated for the most probable value r_1.

Now, in order to determine the *distortion of the lattice positions themselves* we have to separate the effect of thermal vibrations around the positions of individual atoms. The calculated $H_p(r-r_p)$ would then be given by

$$H_p(r-r_p) = H_l(r-r_p) * H_{\text{th}}(r) \tag{16}$$

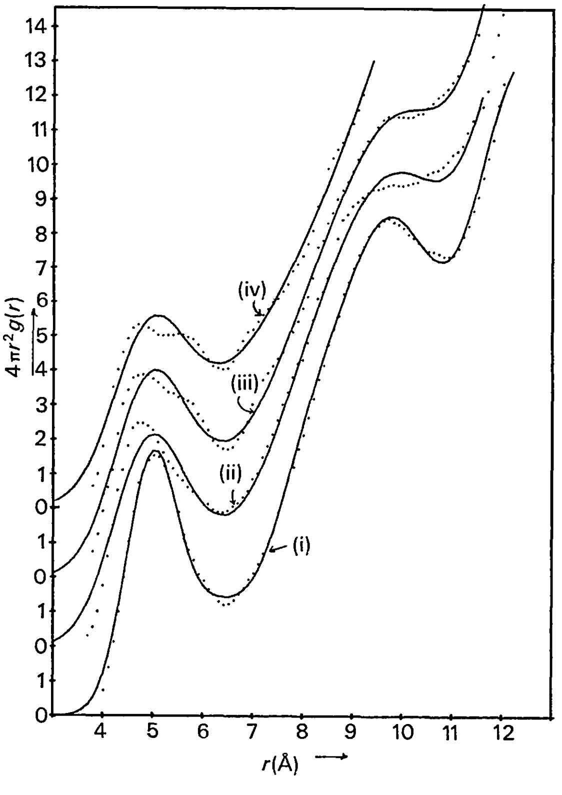

Fig. 7. Liquid rubidium. (i) at 313 °K, (ii) at 433 °K, (iii) at 513 °K, (iv) at 633 °K. Vertical scales are successively by 2 units. Experimental values (. . .) (Gingrich & Heaton, 1961) and calculated (—) RDF by varying all parameters *simultaneously.*

Table 5. *Data as for Table* 3 *but for liquid alkali metals* (*b.c.c. structure*) *at different temperatures*

For the exact meaning of the symbols and their derivation see text (§ 3).

	Li (450 °K)	Na (373 °K)	K (368 °K)
r_1; C_1	3·117; 8·37	3·789; 8·628	4·518; 7·039
r_2; C_2	3·98; 7·25	4·93; 6·65	5·47; 6·74
r_3; C_3	5·18; 11·08	6·25; 10·41	7·25; 7·80
r_4; C_4	5·89; 16·66	7·22; 23·10	9·17; 19·72
r_5; C_5	6·27; 11·67	7·81; 7·20	8·31; 10·76
r_6; C_6	7·32; 14·08	9·59; 5·93	10·39; 8·52
r_7; C_7	7·90; 17·43	9·04; 23·93	12·68; 29·06
r_8; C_8	7·62; 19·53	9·99; 23·44	11·29; 28·20
$\sum^2$	3·18	1·80	2·19

Table 5 (*cont.*)

	Rb								Cs					
	313 °K		433 °K		513 °K		633 °K		303 °K		573 °K		848 °K	
r_1; C_1	4·925;	9·189	4·741;	8·275	4·763;	8·02	4·77;	7·97	5·284;	8·961	5·251;	7·39	5·251;	6·45
r_2; C_2	6·20;	5·18	5·79;	5·73	5·86;	5·98	6·09;	6·17	6·90;	5·03	7·00;	7·55	7·03;	7·21
r_3; C_3	7·99;	10·99	7·95;	12·16	7·94;	11·93	7·95;	11·79	8·79;	10·99	9·02;	11·40	9·98;	11·97
r_4; C_4	9·96;	24·26	9·59;	23·82	9·76;	23·87	9·94;	24·17	10·23;	24·60	11·38;	23·85	11·72;	24·19
r_5; C_5	9·08;	8·72	9·69;	7·96	9·61;	7·83	9·85;	8·07	11·81;	7·74	9·91;	8·58	8·63;	7·09
r_6; C_6	12·48;	5·93	12·34;	6·12	12·60;	6·29	11·06;	5·92	12·55;	5·12	12·83;	5·88	12·86;	6·13
r_7; C_7	11·95;	23·57	12·71;	23·85	12·60;	24·01	12·03;	23·40	13·33;	21·39	14·27;	24·90	16·24;	14·96
r_8; C_8	13·22;	26·24	12·44;	24·08	12·67;	24·01	13·01;	21·88	13·72;	23·39	14·11;	23·94	14·01;	25·41
r_9; C_9			13·79;	23·60	13·60;	23·67	13·68;	24·00			15·26;	24·14	15·63;	20·25
Σ^2	3·50		11·58		6·21		5·83		4·19		3·09		2·20	

where $H_l(r-r_p)$ denotes the normalized distribution function for the lattice positions whose most probable position is given by r_p and $H_{\rm th}(r)$ denotes the corresponding normalized spherically symmetric distribution function due to *harmonic* thermal vibration around *each* of the lattice positions.

Consequently, the lattice distortion due to H_l is given by

$$\Delta^2 a = \Delta^2 r - \Delta^2 s\ . \qquad (17)$$

$\Delta^2 a$, $\Delta^2 s$ are the corresponding mean square displacements in any direction due to H_l and $H_{\rm th}$ respectively. For calculating $\Delta^2 s$ we have used the well known formula in Debye's theory of specific heat, namely

$$\Delta^2 s = \frac{3h^2 T}{4\pi^2 mk\Theta^2}\cdot\left[(\Phi(\xi)+\xi/4\right] = \frac{144{\cdot}5T}{A\Theta^2}\cdot\Lambda\,, \qquad (18)$$

where m is the mass of the atom whose atomic weight is A, h and k are Planck and Boltzmann constants, T and Θ are the Kelvin and Debye temperatures and $\xi=\Theta/T$; $\Lambda=\Phi(\xi)+\xi/4$,

$$\Phi(\xi)=\frac{1}{\xi}\int_0^{\xi}\frac{y\,dy}{\exp(y)-1}\,. \qquad (19)$$

In determining the interaction zone of the lattice, $|p_l|$, which must be distinguished from the correlation length $|p_c|$ of the $g(r)$ function, we have used the formula, [*cf.* also equation (72) of reference II; also equation (13)],

$$|p_l|\simeq(r_1/\Delta a)^2, \qquad (13a)$$

since in this case we do not need the parameter ε. For liquid-like reflexions the size of the lattice must exceed the volume corresponding to this neighbour distance $|p_l|$ ($=d$ Å, say). The linear dimension of the lattice is then given by $L\simeq 2d$ Å. A perusal of the Tables 1 and 2 would show that the correlation length L_c of the $g(r)$ function, as expected from the experimental curves, lies between 10 and 25 Å, whereas the linear dimension of the cluster L varies from 50 to 150 Å.

The values for argon lie in between those for f.c.c. metals and b.c.c. metals.

It should be noted that we have used one distribution function to fit the experimental $g(r)$ curve. This means that we have assumed a statistically homogeneous system. The excellent agreement with the experimental curve shows that near the melting point the clusters, if present in the liquid state, are densely packed so that one set of statistics suffices to explain diffraction data, (see Figs. 3–8). The statistical inhomogeneity of liquid systems assumes importance as we increase the temperature as shown by Figs. 3 (ii), 7 (iii), 7 (iv) and 8 (ii). Further, Fig. 8 shows that the system tends to become again statistically homogeneous corresponding to the gaseous state as we increase the temperature sufficiently. We could not reproduce the second maximum of the experimental curve of argon-2 (91·8 °K and 1·8 atmosphere) reported by Eisenstein & Gingrich (1942) by this method [*cf.* Fig. 3(ii)]. The same also applies to the case of Cs at 573 °K, [*cf.* Fig. 8 (ii)]. Obviously, this strongly suggests that here the distribution of the centroids of clusters themselves plays a significant role in determining the nature of the $g(r)$ functions. In principle this could be corrected by introducing two *a priori* sets of statistics, one due to the first neighbours inside a cluster and the other due to that of centroids of clusters themselves. But we have not yet tried this method. Thus the detailed analyses of $g(r)$ functions, *if properly carried out*, show convincingly that liquids are nothing but distorted crystallites of ultramicroscopic dimensions. Nevertheless, the excellent agreement between the theoretical and experimental curves in the densely packed systems does not necessarily mean that liquids near melting points are statistically homogeneous systems consisting of only one large generalized lattice as has been assumed implicitly by the present method of analysis of $g(r)$ curves. In order to justify our assumption that it is really a densely packed heterogeneous system, (on the atomic scale), we need to study more carefully the theoretical $g(r)$ – functions calculated from the distribution function theory of statistical mechanics and the various properties of the system related to it.

4. Evidence for the existence of clusters in the liquid state

In order to offer convincing evidence for the existence of clusters at the melting point, though a RDF calculated from the assumption of the existence of a single homogeneous lattice agrees well with the observed function, we shall discuss here the case of liquid argon and liquid sodium. Khan (1964) had calculated theoretical $g(r)$ curves of argon at several temperatures (from Percus–Yevick and CHNC integral equations) by using the superposition approximation of the Kirkwood and Lennard-Jones potential as well as the Guggenheim–McGlashan potential. Most of his computed curves differ *even qualitatively* from the observed curves reported by Eisenstein & Gingrich (1942). For example, for argon at 144·1 °K and number density $1{\cdot}3/2\times10^{-2}$ per Å^3 the computed curves are much wider and the second maximum occurring at 5·2 Å in the experimental curve is completely missing. Even at 91·8 °K, the experimentally observed second maximum is not reproduced in the theoretical curve. It is interesting to note that we also could not get this maximum from the assumption of a homogeneous lattice. But Kahn's calculated curve using the LJ potential and the PY method agrees quite well with the experimental curve for argon at the triple point. Since the conclusions derived from statistical mechanical considerations are certainly correct for homogeneous systems containing a sufficiently large number of atoms, one could expect that the properties of argon at the triple point calculated from such $g(r)$ values would also agree well with the observed properties. But the calculated values of pressure and compressibility as reported by Khan differ from the observed values by orders of magnitude. Certainly such a large discrepancy cannot be ascribed either to the inadequacy of the superposition approximation or to the inaccuracy in the values of the parameters of the potential function. If this were so, we would not get such nice agreement for the $g(r)$ curves. In particular, the calculated and experimental values of isothermal compressibility which depend only on $g(r)$ and not on the interacting potential ought to agree equally well also. Further, other properties like viscosity and surface tension which, like pressure, depend on the slope of the potential function would differ similarly. But the results reported by Johnson, Hutchinson & March (1964) show that calculated values agree fairly well with the experimental values.* Since we cannot doubt the validity of statistical mechanics for large homogeneous systems, the only logical and consistent inference from these discrepancies is the hypothesis that the system consists of densely packed small clusters. Our conviction of the legitimacy of our conclusion is further strengthened by the fact that although the experimental and calculated $g(r)$ functions for the case of liquid sodium at 373 °K agree extremely well [see Fig. 6 (ii)], values of pressure and isothermal compressibility calculated by using the oscillating potential function given by Johnson *et al.* (1964) also differ by orders of magnitude from the corresponding experimental values. This again must be ascribed to the presence of clusters, since the pair potential was calculated from the observed $g(r)$.

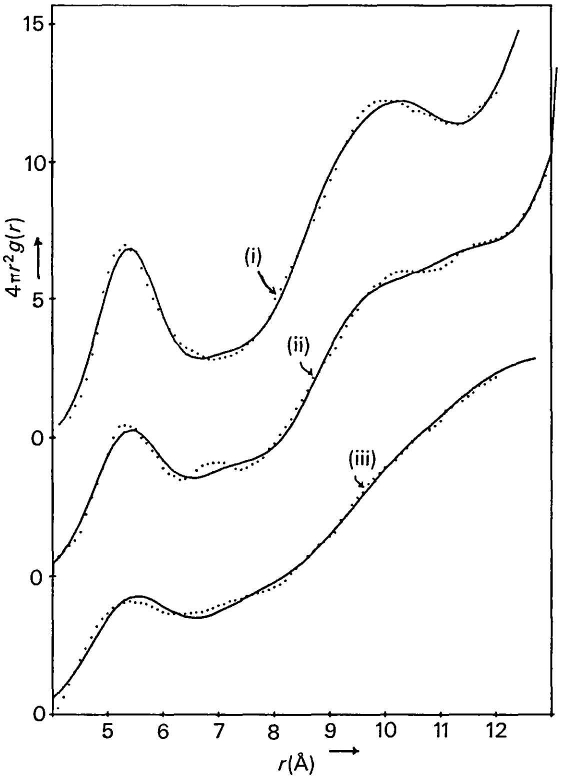

Fig. 8. Liquid caesium. (i) at 303 °K, (ii) at 573 °K, (iii) at 848 °K. Vertical scales are successively shifted by 5 units. Experimental values (. . .) (Gingrich & Heaton, 1961) and calculated (—) RDF by varying all parameters *simultaneously*.

Thus quantitative and comparative studies of the RDF lead us to the only acceptable conclusion:

At the triple point or near the melting point the dense systems behave almost as a statistically homogeneous entity, *i.e.* the distribution function for the locations of different atoms with respect to a fixed origin is practically homogeneous. Actual inhomogeneity of the systems is revealed by those properties like pressure and compressibility which are sensitive to the presence of clusters.

At higher temperatures, the clusters are separated by relatively much larger distances so that the distribution functions for the location of different neighbours depend on the choice of the origin and we get only the ensemble average in which the average properties of the individual members of the ensemble, *e.g.* clusters, 'cybotactic groups' are lost and cannot be retrieved from the observed $g(r)$ functions without further analysis (*e.g.* from the standpoint of statistical me-

---

* For viscosity this is true for the Born–Green method. The value calculated by the PY method is 30 times less than the experimental value.

chanics of small systems) and perhaps some additional plausible hypotheses.

5. Absence of observable small-angle scattering

It is perhaps worthwhile to say a few brief words of explanation of the absence of small-angle scattering in diffraction diagrams of liquids near their melting points in spite of the presence of clusters of linear dimension 50–150 Å, since the tails of 000 reflexions of such clusters would extend up to $\sim 1^\circ$.

The reasons for the absence of any noticeable effect of such small clusters in densely packed systems are mainly twofold: first, the intensity of 000 reflexions in the region of experimental studies would be much too weak to be recognized easily. It should be kept in mind that the overall appearance of small-angle scattering, as is well known (*cf.* Guinier & Fournet, 1955; Levelut & Guinier, 1965), depends on the size of the clusters, their density of packing and on the contrast of the density $(\rho_c-\bar{\rho})^2$. ρ_c is the actual density within the cluster itself and $\bar{\rho}$ the average (macroscopic) density of the system. If the size of the clusters decreases, the small-angle scattering becomes broader and consequently the intensity decreases. Further, for densely packed systems the density contrast would also be quite small.

But the chief reason for the absence lies in the atomic arrangement of dense systems. RDF analysis shows that the average distances between two nearest neighbours in adjacent clusters do not differ by more than 3% from those in a crystal at the same temperature, a small value compared to their dispersions, (10–12%). Consequently, one can safely conclude that such systems, so far as diffraction data are concerned, behave *as if* they form single homogeneous lattices, the only difference being a slight increase in the backgroundscattering due to a slightly greater $\Delta^2 N$.*

6. Significant structure model of the liquid state in the light of the unified theory of diffraction

Of all model theories of the liquid state, the significant structure theory has been extremely successful in explaining thermodynamic properties of many liquids near melting temperatures (*cf.* Eyring, Ree & Hirai, 1958; Eyring & Marchi, 1963). This theory visualizes liquids as a mixture of crystals and gases, their relative concentration being determined by the excess volume at the melting point. Consequently the liquid partition function is given by the product of known crystalline and gaseous partition functions. Using a few plausible assumptions Eyring and his coworkers obtained an expression for the partition function of the liquid in which only macroscopically observed parameters are involved. In spite of the remarkable agreement between calculated and observed values, this theory has not received adequate attention from theoreticians, presumably because of the fact that it contains too many *ad hoc* assumptions. Further, the assumption of simultaneous existence of two phases, one consisting of a large ideal single crystal in the liquid state, is obviously physically untenable. Nevertheless, the concrete achievements of the theory force us to try to understand why this model succeeds. Presumably the success is due to the fact that this model, though not in its literal sense, reflects the actual nature of the liquid state. As shown below, from the standpoint of diffraction theory this model is completely equivalent to the concept of the liquid state at which we had arrived previously. The only difference lies in the fact that in our case the crystallites are distorted microcrystallites and there is no need to postulate the simultaneous existence of the two phases, although a few molecules may be roaming about in the intercluster space.

In order to prove this, it suffices to note that our system may be *looked upon* as a very large distorted crystal embedded with agglomerated point defects. As Levelut & Guinier (1965) have shown, the inter-

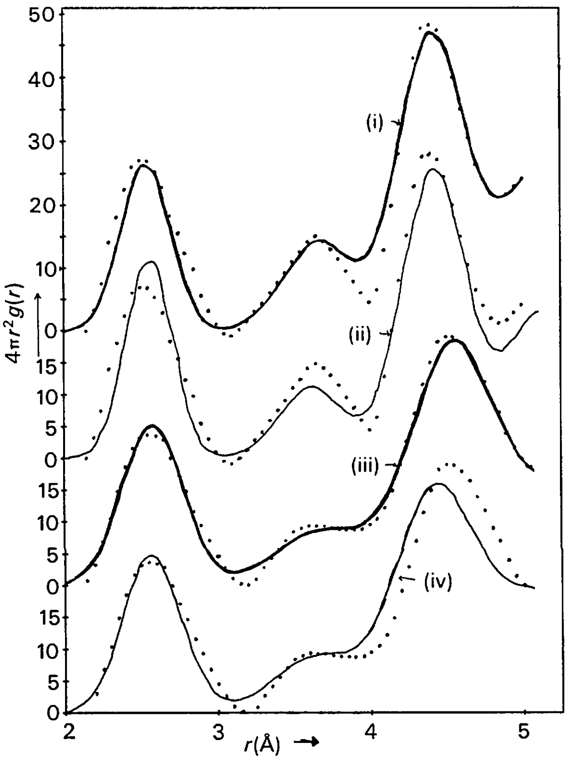

Fig. 9. Solid copper (Ruppersberg, 1966). (i) at 973 °K by varying all parameters simultaneously, (ii) at 973 °K by varying only α, (iii) at 1293 °K by varying all parameters, (iv) at 1293 °K by varying only α. Vertical scales are successively shifted by 20 units.

---

* This slight inhomogeneity can nevertheless have appreciable effect on the relative motion of the individual atoms and the centroids of the clusters themselves. Thus, it is expected to influence the pressure, compressibility, diffusion coefficients and electronic properties of such systems.

ference effect of such a system would produce in addition to the usual diffraction patterns of such (distorted) crystals, a continuous scattering I_g due to these vacancies where

$$I_g = cv|f_0|^2. \tag{21}$$

Here c is the concentration of vacancies segregated into v groups and $|f_0|^2$ is the structure factor of the atom in the crystal. This means that the scattered intensity of the system containing N atoms is practically the same as that given by a mixture of a (distorted) crystal containing $(N-N_g)$ atoms and N_g $(=cv)$ atoms of the same substance existing as gas molecules.

7. Summary

For convenience we summarize here the major conclusions arrived at above.

(i) In order to arrive at practically useful results, all theories of diffraction have to introduce the concept of probability of the distribution of scattering centres. That means that the system is supposed to be a statistically homogeneous entity.

(ii) Even at ordinary temperatures *real* crystals do not form *ideal* periodic lattices. Such systems can be adequately described with the help of a generalized lattice in which the centroids of atoms are distributed randomly around their most probable positions. Thus the anharmonic effect of thermal vibrations can be separated into such a distribution H_l of the centroids of the atoms and a harmonic vibration H_{th} around each of these centroids, *analogous* to the so-called quasi-harmonic case of ideal crystals.

(iii) With increasing temperature lattice distortion increases and near the melting point it becomes quite significant and changes discontinuously to the value for the liquid state.

(iv) The liquid state consists of distorted microcrystallites. Relative lattice distortion in general is around 10% for f.c.c. structures and 8% for b.c.c. structures. The estimated linear dimension of the clusters varies from 50 to 150 Å, depending on the type of crystalline structure. With increasing temperature the lattice distortion increases and the size of the clusters decreases.

(v) A first-order phase transition is governed principally by the condition that a statistically homogeneous distribution function becomes inhomogeneous. Crystals and gases present homogeneous distributions for the probabilities of occurrence of the neighbours, but in the liquid state they are inhomogeneous.

(vi) The absence of (detectable) small-angle scattering of liquid systems near their melting points does not necessarily mean that small clusters do not exist in the system. Quantitative and comparative studies of $g(r)$ functions calculated from the distribution function theory of statistical mechanics for liquid argon and liquid sodium lead to the *inevitable* conclusion that liquids near melting points are densely packed systems of small clusters. For the liquid state one must study statistical thermodynamics of small systems.

(vii) The striking success of the significant structure theory of the liquid state is explained satisfactorily in terms of the existence of these clusters of distorted crystallites.

References

Bagchi, S. N. (1970). *Advanc. Phys.* **19**, 119.
Eisenstein, A. & Gingrich, N. S. (1942). *Phys. Rev.* **62**, 261.
Eyring, H. & Marchi, R. P. (1963). *J. Chem. Educ.* **40**, 562.
Eyring, H., Ree, T. & Hirai, N. (1958). *Proc. Natl. Acad. Sci. U.S.A.* **44**, 683.
Gingrich, N. S. & Heaton, L. (1961). *J. Chem. Phys.* **34**, 873.
Gingrich, N. S. & Thompson, C. W. (1962). *J. Chem. Phys.* **36**, 2398.
Guinier, A. & Fournet, G. (1955). *Small Angle Scattering of X-rays*. New York: Wiley.
Hendus, H. (1947). *Z. Naturforsch.* **2**A, 505.
Henshaw, D. G. (1957). *Phys. Rev.* **105**, 976.
Hosemann, R. & Bagchi, S. N. (1962). *Direct Analysis of Diffraction by Matter*. Amsterdam: North Holland.
Johnson, M. D., Hutchinson. P. & March, N. H. (1964). *Proc. Roy. Soc.* A**282**, 283.
Kaplow, R., Averbach, B. L. & Strong, S. L. (1964). *J. Phys. Chem. Solids*, **25**, 1195.
Kaplow, R., Strong, S. L. & Averbach, B. L. (1965). *Phys. Rev.* **138**, A1336.
Khan, A. A. (1964). *Phys. Rev.* **134**, A367.
Levelut, A. M. & Guinier, A. (1965). *In Small-Angle Scattering*, edited by H. Brumberger. New York: Gordon & Breach.
Ruppersberg, H. (1964). *Mem. Sci. Rev. Metall.* **LXI**, 709.
Ruppersberg, H. (1965). Z. *Naturforsch.* **20a**, 104.
Ruppersberg, H. (1966). Z. *Phys.* **189**, 292.
Sharrah, P. C. & Smith, G. P. (1953). *J. Chem. Phys.* **21**, 228.
Zernike, F. & Prins, J. A. (1927). *Z. Phys.* **41**, 184.